aerospace

MDPI

Article

Impact of Mega Constellations on Geospace Safety

Haicheng Tao, Qinyu Zhu, Xueke Che, Xinhong Li *, Wanxin Man, Zhibin Zhang and Guohui Zhang

Department of Aerospace Science and Technology, Space Engineering University, Beijing 101416, China; homerthc@foxmail.com (H.T.); qyzhu97@foxmail.com (Q.Z.); hrche2021@163.com (X.C.); manwanxin@126.com (W.M.); zhangzhibinseu@163.com (Z.Z.); zhangguohui123@stu.xjtu.edu.cn (G.Z.)
* Correspondence: 13366159269@189.cn

Abstract: The extent of the impact of mega constellations on the low-orbiting geospace environment, which has not yet been assessed in more concrete quantitative terms, is an extremely important issue to consider as mega constellations are built. Satellite safety and lifetime can clearly represent the situation of space targets, and thus can reflect the impact of mega constellations on geospace security. Three target satellites with different characteristics were selected and the Accepted Collision Probability Level (ACPL) was calculated to obtain the impact of Starlink on satellite mission lifetime. Upon considering Starlink without early avoidance control, the lifetimes of the three target satellites were shortened by 56.21%, 99.09%, and 99.82%, respectively. After 10 revolutions of early avoidance control, two were shortened to 92.166% and 91.99%, while the lifetime of JILIN-01 was extended by 155.44%. After joining Starlink, the total risk became larger; even if the target satellite avoided control far more frequently than before joining Starlink, it will face a worse geospace environment. Adopting the most aggressive orbit avoidance control cannot avoid the deterioration of the geospace environment from the perspective of satellite lifetime, which is an irreversible and deteriorating process.

Keywords: *mega constellation*; *geospace environment*; accepted collision probability level; *satellite lifetime*

Citation: Tao, H.; Zhu, Q.; Che, X.; Li, X.; Man, W.; Zhang, Z.; Zhang, G. Impact of Mega Constellations on Geospace Safety. *Aerospace* **2022**, *9*, 402. https://doi.org/10.3390/aerospace9080402

Academic Editor: Paolo Tortora

Received: 5 June 2022
Accepted: 23 July 2022
Published: 26 July 2022

1. Introduction

The Federal Communications Commission (FCC) approved OneWeb LLC's entry into the US market using its proposed NGSO FSS (fixed satellite service) on 22 June 2017. OneWeb had previously stated that it planned to launch 720 satellites in 2018 [1]. According to the FCC report, SpaceX plans to eventually launch 42,000 Starlink satellites [2]. Likewise, E-Space plans to begin deploying a constellation of 100,000 satellites in 2022 [3], China's spectrum allocation dossier to the International Telecommunication Union (ITU) in 2020 includes two broadband constellation plans called GW-A59 and GW-2 [4], the FCC has approved Amazon's Kuiper constellation [5], and Samsung has announced plans for a mega constellation for the Internet in Space [6], the details of which are given in Table 1; all of these efforts indicate a future in which low-orbit space will be filled with satellites. As shown in Figure 1, the mega constellation plans of various countries have resulted in a dramatic increase in the number of satellites launched in a calendar year, as well as a dramatic change in the Earth's low-orbit space environment. The most obvious impact on the space environment is space safety, and the dense number of mega constellations has resulted in frequent close approach events. All currently planned LEO mega constellations are expected to receive a large number of collision warnings, as any predicted approach distance of less than 20 km could result in control avoidance [7].

Table 1. Major international mega constellation programs [1,3–6,8,9].

Name	Affiliation	Altitude [km]	First Launch Data	Number of Satellites
Starlink	SpaceX	340–1150	24 May 2019	41,927
E-Space	E-Space	LEO	March 2022	100,000
Kuiper	Amazon	590–630	No launch	3236
OneWeb	OneWeb	1200	27 February 2019	1980
Space Internet	Samsung	2000	No launch	4700
GW-A69	China Star Network	508–590	No launch	6080
GW-2	China Star Network	1145	No launch	6912

In terms of mega constellation impact on the Earth's space environment, Radtke et al. discovered that the first-generation OneWeb constellation had a 35% probability of catastrophic collisions over the mission lifetime [10]. Over a 90-day period, Reiland et al. discovered 522 close encounters of less than one kilometer in the OneWeb constellation, with a minimum distance of only 6.4 meters, and 3676 close encounters of less than one kilometer in the Starlink constellation's five orbital planes combined, with a minimum approach distance of 16.7 meters [11]. According to Anselmo et al. that full compliance with the Inter-Agency Space Debris Coordination Committee (IADC) mitigation guidelines and the 25-year rule will enable long-term control and basic stabilization of the LEO debris environment [12]. Given a 10% failure rate for end-of-mission disposal or satellite failure, this is still possible, but higher failure rates, such as those documented by LEO (50–60%), will result in a significant increase in debris [13], while the number of objects on LEO has been increasing due to the excessive failure rate and frequent launch activity over the year. The evolution of LEO-catalogued objects according to data on CeleTrak [14] is shown in Figure 2. Luciano Anselmo et al. introduced a specific critical index of collision rate percentage growth to assess the environmental impact of large satellite constellations in near-Earth orbit [15]. The results of this index, which was calculated for various constellations and applied at altitudes ranging from 800 km to 1400 km, show that in regions of space where the current catalogued debris density is already high, such as around 800 km, adding 100 more abandoned satellites would increase the current collision rate by about 10%; in less-crowded low-orbit regions, such as near 1110 km and 1325 km, adding 100 more abandoned satellites would increase the current collision rate by about 10%; and in less-crowded high-orbit regions, such secondary collisions from mega constellation satellites are also a significant threat to the Earth's geospatial environment, according to Tao et al., with the probability of collision for surrounding orbiting satellites exceeding the red alert threshold of 10^{-4} within 30 min of a mega constellation satellite collision [16]. Oltrogge et al. found that the situation in LEO space is not yet dire if properly managed; however, both LEO and GEO have substantial and persistent collision risks, and these collision risks, along with debris events, pose far-reaching and long-lasting effects [17]. Muelhaupt et al. characterized NewSpace as a dramatic change in the space environment with the launch of mega constellations, and in order to cope with the changes brought about by NewSpace, it is crucial to reconsider how to develop new space environment management programs and enhance all aspects of space traffic management [18]. Lewis et al., Kawamoto et al., and Anselmo and Pardini point out that [19–21] strict adherence to post-mission disposal guidelines and disposal at the end of a satellite's expected operational life, where possible [22], is critical to mitigate the impact of these mega constellations on the near-Earth geospace environment. However, as noted above, the current disposal success rate is no more than 50 percent. According to CelesTrak forecasts, Starlink is the satellite with the nearest rendezvous events in LEO space, with a total of 224 near approach events with a collision probability exceeding the red alert limit of 10^{-4} within 7 days for Starlink launches as of 10 April 2022, the majority of which are its own rendezvous events with itself,

but there were also many rendezvous with other LEO satellites. These findings suggest that mega constellations have a significant impact on the geospace environment of LEO satellites, raising the question of how to quantify such impact and assess visual impact on LEO satellites.

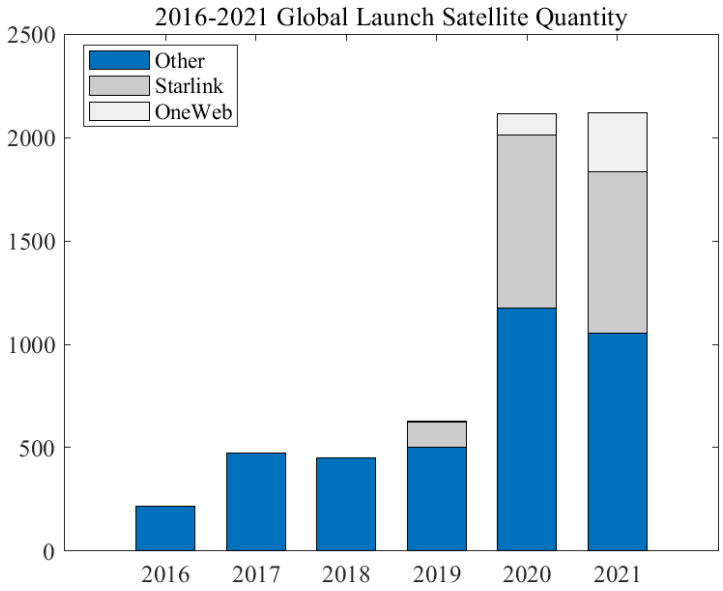

Figure 1. Number of satellites launched over the years [23].

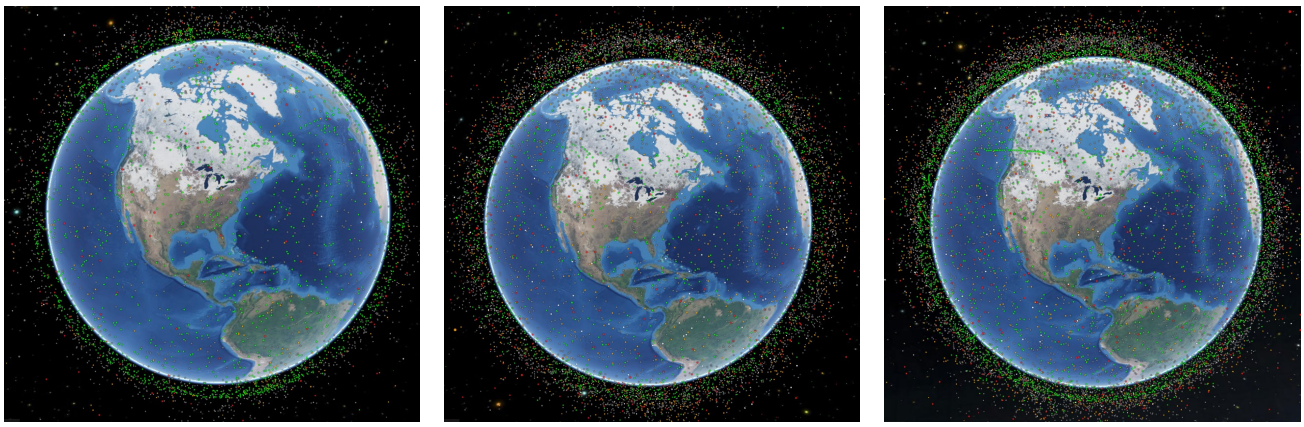

(**a**) (**b**) (**c**)

Figure 2. Changes in space catalogued objects in LEO, (**a**) 2000 (**b**) 2010, (**c**) 2022 [14].

The impact of mega constellations on low-orbiting satellites has been well-documented, with the European Space Agency (ESA) maneuvering an Earth science satellite, Aeolus, to avoid a potential collision with the Starlink 44 satellite in 2019 [24]. According to a document provided by China to the UN space agency in December 2021, the Starlink satellite flew dangerously close to the Chinese space station on two occasions, for which the Chinese space station has implemented two avoidance control measures [25]. The presence of many other spacecraft in Earth's near-Earth orbit, which is also affected by mega constellations for orbital safety, and the orbital maneuvering of satellites to avoid collisions (which requires the consumption of propellant and therefore reduces the satellite's lifetime), is posing a challenge to normally operating satellites in the same orbit in order to avoid collisions with them. The geospace environment is changing dramatically as a result of the emergence of mega constellations, and the extent of this change is an urgent concern for the future; this paper aims to discuss the solution to this problem as well as provide its own approach.

Mega constellations have already had a significant impact on the geospace environment of low-orbiting satellites, but this type of impact has not been well-quantified. In this paper, Starlink is used as a mega constellation and three target satellites with different characteristics are chosen to calculate the impact of Starlink on Earth's LEO space in order to better quantify this impact and determine which characteristics are most affected. While two cases exist, only one without considering Starlink i.e., only other satellites, exists. The other one, which considers Starlink's first-batch distribution plan, is combined with MASTER calculations in consideration of the Alt-V and Alt-Mass orbital flux changes of the three LEO satellites before and after Starlink. It seeks to obtain the impact of Starlink on the flux changes of the Earth's space environment, calculate its impact on the ACPL values of LEO satellites and the orbital maneuvers required for LEO satellites ΔV and the propellant mass fraction (PMF), and calculate the change in mission lifetime of the target satellite to quantitatively assess the impact of the mega constellation on the LEO satellite geospace environment in terms of satellite mission lifetime and safety.

2. Models and Assumptions

2.1. Orbital Flux Calculation and Collision Probability Model

The MASTER-8 model flux calculation utilizes a similar approach to gas dynamics theory, where space debris travels through the particle-filled Earth space environment as if the surface were sweeping through a static gas-filled space container, called a "bin", as depicted in Figure 3. As shown below, Earth orbital space is divided into an infinite number of similar space containers, with Δh indicating the container height, $\Delta\alpha$ the container longitude span, and $\Delta\delta$ the latitude span.

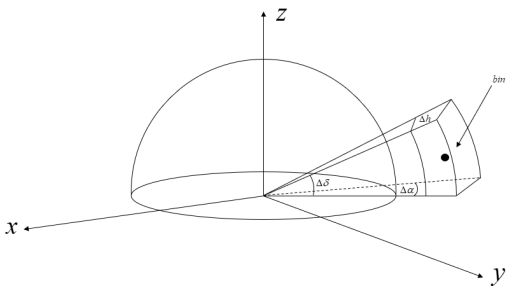

Figure 3. The spatial pattern of the bin.

The total space flux is describef by Equation (1)

$$F = \sum_i F_i = \sum_i (\sum_{bin} q_{bin} \times p_t \times \Delta v_p) \tag{1}$$

F_i denotes the flux within a single space, q_{bin} denotes the spatial density at rest, p_t means the target residence probability within the "bin", and Δv_p denotes the relative velocities of space objects and static objects. The flux distribution of the spacecraft's operational orbit can be obtained from the evolved orbital object distribution, and Equation (2) can be applied to determine the average number of collisions n [10].

$$n = F \times A_c \times T \tag{2}$$

F is the flux, calculated from MASTER-8, T is the time frame, and A_c is the cross-sectional area of the collision, which in this paper is the cross-sectional area of the Starlink satellite in orbit.

From the average number of collisions n, collision probabilities can be calculated using Poisson statistics, m means the number of times a collision event occurs.

$$P_{i=m} = \frac{n^m}{m!} e^{-n} \tag{3}$$

2.2. ACPL Assessment Model

The probability of collision is an important factor to consider when deciding whether to perform an avoidance maneuver. In this regard, determining the threshold probability to be applied to trigger maneuvers is critical. If this threshold is set too high, a large number of approach points will be ignored, exposing the operator to significant risk throughout the mission's duration. If the threshold is set too low, however, the number of operation tasks may be excessive, with the majority avoiding only a minor overall risk. In this paper, the ACPL (accepted collision probability level) value is selected as the index of this threshold. ACPL is the relationship between the number of avoidance times and collision risk, and represents the average number of avoidance maneuvers with acceptable collision probability [15].

ESA developed DRAMA to assist with threshold selection (Debris Risk Assessment and Mitigation Analysis) [26]. We primarily employ its ARES (Assessment of Risk Event Statistics) module for the assessment in this paper, and we use DRAMA to calculate the ACPL using collision probability obtained through the above equation, adding the Starlink constellation to the race group of DRAMA to obtain the degree to which the target satellite is affected by Starlink. According to current research for RapidEye constellation, the more acceptable ACPL value is 10^{-4} [15].

If the ACPL-10^{-6} is chosen, the residual risk can be reduced to zero when only known objects are considered, but it also implies a large number of avoidance maneuvers, which is unacceptable for in-orbit satellite mission lifetimes, so the ACPL value of 10^{-4} is generally chosen. The computational model is shown below.

If the spacecraft is maneuvered when the collision risk from the catalog object exceeds the acceptable level, the associated collision avoidance maneuver rate can be determined based on the passage rate (i.e., flux) of the catalog object in the elliptical region as we determine, as shown in Equation (4), and the velocity increments given later ΔV and the propellant mass fractions based on different ACPL worthy avoidance maneuvers are calculated.

The concept of collision risk is shown in Figure 4. As shown below, the collision cross section is defined as an elliptical surface divided into an infinite number of microelements, and dA denotes a microelement in this surface [27].

$$\dot{N}_c = \sum_{j=1}^{J} \int_0^{A_j(P_{c,acc})} F dA \quad j = 1, 2, 3 \ldots J \tag{4}$$

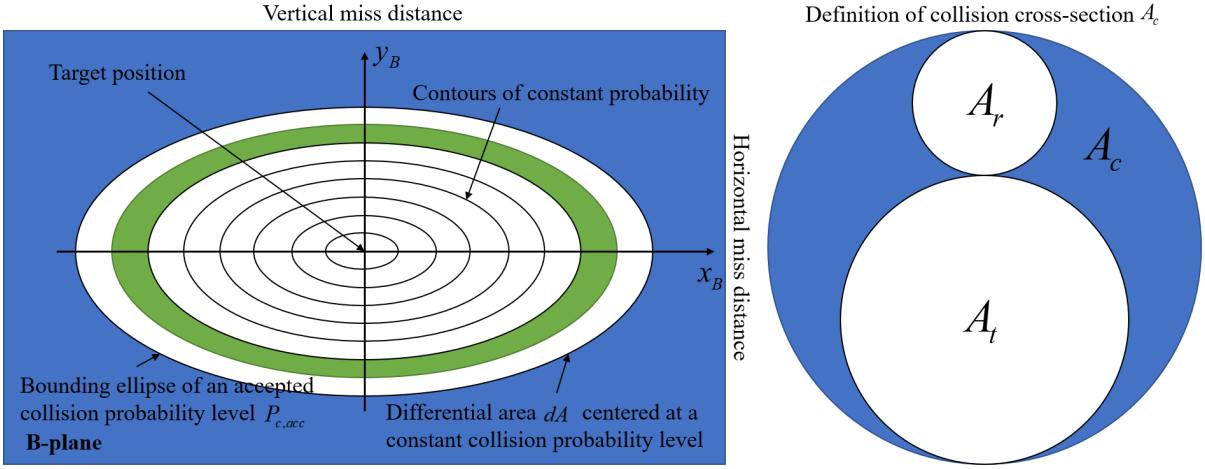

Figure 4. Illustration of the concept of collision risk estimation based on the integration of statistical object fluxes over a collision probability density function in the b-plane centered on the target object.

$P_{c,acc}$ represents the acceptable collision level, i.e., ACPL, $\dot{N}_c$ denotes the number of collision avoidance control, and the number of avoidance control operations is calculated according to $P_{i=m} > P_{c,acc}$. In order to ensure that the satellite safety level is acceptable, the ACPL is generally selected as 10^{-4}, which corresponds to the red warning threshold [28].

A_j denotes the sum of the collision area of different objects with orbiting satellites, i.e., the cross-sectional area of the Jth target object A_c, $A_c = (\sqrt{A_t} + \sqrt{A_r})^2$, A_r denotes the cross-sectional area of orbiting satellites, A_t indicates the cross-sectional area of different objects, and F denotes the sum of the fluxes of all target objects (in this paper, i.e., the different fluxes of the orbit with and without Starlink).

2.3. Starlink Constellation Configuration and Selection of Target Satellites

2.3.1. Starlink Constellation Configuration

According to the FCC report SAT-MOD-20200417-00037 [8], the summary of the NGSO (Non-Geostationary-Satellite Orbit) constellation after the star chain modification can be obtained as Table 2. As shown in the table, it can be seen that a total of 4408 satellites will be deployed in the vicinity of 550 km orbit. To simplify the calculation, it is assumed that the satellites' orbits do not change during the calculated time-period, and their positions are designated according to the table below. 'Orbital planes' means the number of orbital planes, and 'Satellites per plane' refers to the number of satellites in each plane.

Table 2. Starlink Deployment Summary.

Orbital Planes	**72**	**72**	**36**	**6**	**4**
Satellites per plane	22	22	20	58	43
Altitude	550 km	540 km	570 km	560 km	560 km
Inclination	53°	53.2°	70°	97.6°	97.6°

2.3.2. Target Satellite Parameters

Three different types of satellites were selected as target satellites for the calculations, with the aim of assessing the impact on LEO satellites of different volumes, orbital altitudes, and orbital inclinations, with orbital data and satellite parameters from SpaceTrack and DISCOweb, as shown in Table 3. The orbital data for the three satellites were obtained from two rows of SpaceTrack elements TLE [29].

Table 3. Satellite Parameters.

Name	**PERIOD**	**Inclination**	**Apogee**	**Perigee**	**Mass**	**Width**	**Height**	**Depth**
JILIN-01-01 GAOFEN 2D	95.38 min	97.54°	547 km	527 km	230 kg	0.5 m	1.1 m	0.5 m
CORVUS BC5	94.43 min	97.43°	500 km	481 km	10 kg	0.2 m	0.3 m	0.2 m
YAOGAN-35 C	94.54 min	35°	497 km	496 km	300 kg	2.5 m	2.5 m	2.5 m

3. Impact of Starlink on Environmental Fluxes in Earth's low-orbit Space

For low-orbiting satellites, mega constellations lead to significant changes in the flux of objects in the Earth's space environment, which is responsible for the change in collision probability and is fundamental to the satellite avoidance strategy. This paper employs a heat map to illustrate the flux change visually. The top view of the heat map helps us to determine which region of the flux is significantly affected, making it easier to judge the pattern of flux change.

Figure 5 represents the heat map of the flux distribution of object height and impact velocity (Alt-V), the top of each satellite flux heat map is the flux distribution without Starlink, and the bottom is the flux distribution considering Starlink. The figure on the left represents the top view of the heat map, which is a magnified representation of the projection of the heat map in the Alt-V plane, from which it can be more effectively observed that considering Starlink before and after for that region has a greater impact.

Figure 5a,b shows the comparison of Alt-V flux variation of JILIN-01-01 GAOFEN 2D satellite, where the highest point becomes 3.258 $\times$ $10^{-6}/m^2/yr$ at 548.399 km and 11.5 km/s due to the addition of the Mega Constellation Starlink, which is 27.96 times higher than without the addition, as can be seen from the top view. The influence of Starlink is regionalized, being more pronounced for altitude fluxes in the 540 km–550 km range and velocity fluxes in the 14–16 km/s range.

Figure 5c,d shows the comparison of Alt-V flux variation of CORVUS BC5 satellite, which has similar orbital altitude and similar inclination with GAOFEN. The difference is that their satellite masses are very different, the space flux is mainly concentrated between 480–500 km, 8–16 km/s without Starlink, and the distribution is more even; the maximum value is 8.394 $\times$ $10^{-8}/m^2/yr$ at 481 km and 14.5 km/s. After adding Starlink, the space flux is concentrated between 495–500 km and 6–16 km/s, with a more concentrated distribution, and its maximum value becomes 4.647 $\times$ $10^{-5}/m^2/yr$ at 499.452 km and 13.5 km/s, and the latter value becomes 553.6 times the former value. The flux variation of CORVUS BC5 is more concentrated in contrast to the flux variation of GAOFEN, and there is a relationship between this variation and the volume of both.

Figure 5e,f shows the comparison of Alt-V flux variation of YAOGAN-35C satellite. The biggest difference between this satellite and GAOFEN and CORVUS BC5 is the variation of its inclination angle; before considering Starlink, the spatial flux of YAOGAN-35C is evenly distributed in the range of 475–520 km and 8–15 km/s, indicating that the size is more prominent. The maximum value is 1.871 $\times$ $10^{-8}/m^2/yr$ at 505 km, 15.5 km/s. After considering Starlink, the spatial flux distribution becomes concentrated, mainly in the range of 495–510 km, 7–16 km/s, and the prominent values are extremely concentrated and vary greatly. The maximum value becomes 4.001 $\times$ $10^{-5}/m^2/yr$ at 504.2253 km, 11.5 km/s, changing to 2138.428 times the former. The flux variation due to the change in inclination is more pronounced compared to the flux variation due to the change in volume and mass. According to the above cases, the impact on the orbital safety is substantial; the specific and the quantified impact will be analyzed in detail in the following section.

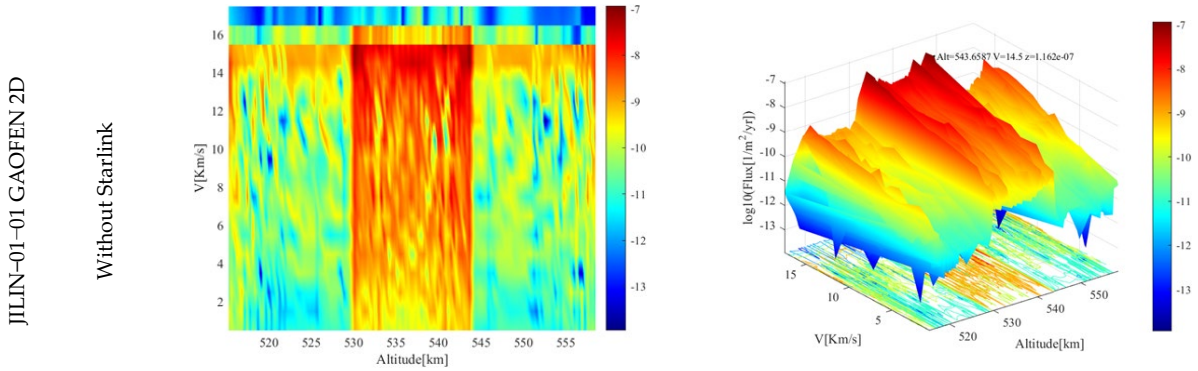

Figure 5. *Cont.*

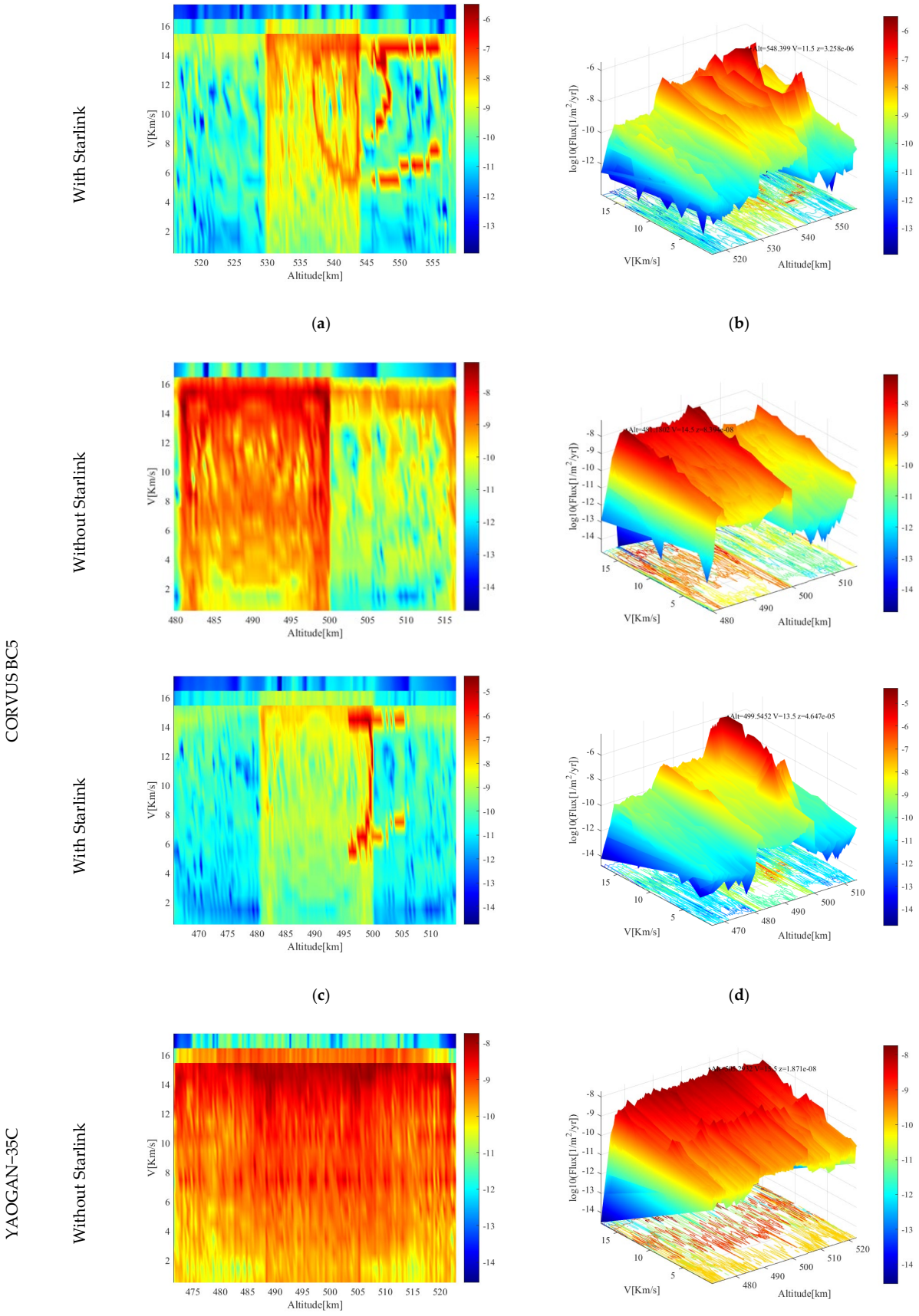

Figure 5. *Cont.*

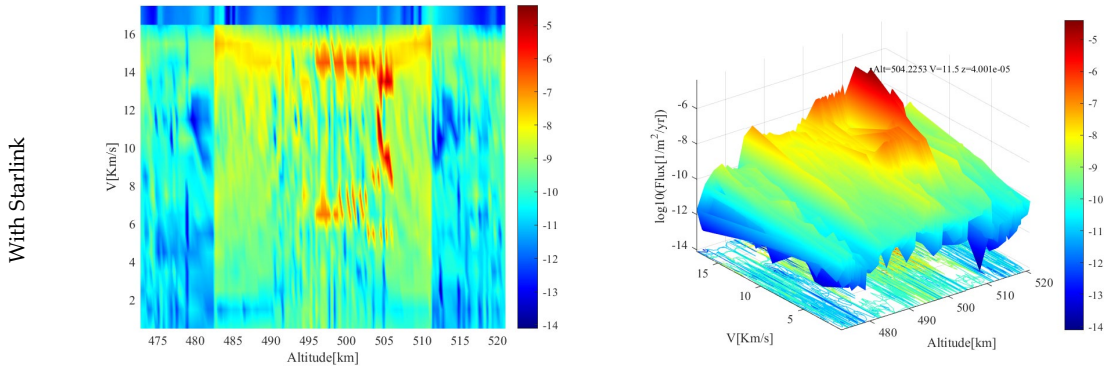

(**e**) (**f**)

Figure 5. Orbital object flux and velocity flux variation. (**a**,**b**) Before and after Alt-V fluxes of GAOFEN satellites; (**c**,**d**) Before and after Alt-V fluxes of CORVUS BC5 satellites; (**e**,**f**) Before and after Alt-V fluxes of YAOGAN-35C satellites.

Figure 6 is a representation of the flux distribution heat map for object height and object mass (Alt-Mass). Similar to Figure 5, the top of each satellite flux heat map is the flux distribution without Starlink, and the bottom is the flux distribution considering Starlink. The figure on the right depicts the heat map of the flux distribution corresponding to the height and mass of various objects, allowing for a clear comparison of the trend of the flux extremes before and after the increment.

Figure 6a,b shows the comparison of Alt-Mass flux variation of JILIN-01-01 GAOFEN 2D satellite, the highest point of flux before Starlink is $1.542 \times 10^{-7}/\mathrm{m}^2/\mathrm{yr}$ at 543.6587 km altitude and 0.6796 kg of mass. In this scenario, the main source of flux is a series of small objects such as space debris in low orbit space. The flux distribution is more even, due to the consideration of the mega constellation Starlink. The highest point becomes $3.874 \times 10^{-6}/\mathrm{m}^2/\mathrm{yr}$ at 548.399 km and 222.6219 kg, which is 25.123 times higher than the former. The top view shows that the flux impact of Starlink is very clustered in a smaller area for altitudes in the range of 535 km. The flux impact is more obvious for the height range of 535–555 km and the mass range of 200–250 kg, and the flux impact is especially strong for the mass of the object around 225 kg, which is related to the properties of Starlink itself. In short, the flux has shifted from a previously uniform distribution to a more concentrated distribution; the precise effect of this change will be explained in the following section.

Figure 6c,d shows the comparison of Alt-Mass flux variation of CORVUS BC5 satellite; compared with the flux variation of Alt-V, the flux variation of Alt-Mass is more concentrated. It is believed that the uncertainty of mass interval is smaller than the uncertainty of Starlink velocity interval; the spatial flux is mainly concentrated in the range of 480–500 km, between 0–450 kg, with a more even distribution, which is more similar to the distribution of Alt-V, with the maximum value of 499.5452 km, 0.67962 of $1.216 \times 10^{-7}/\mathrm{m}^2/\mathrm{yr}$. After considering Starlink, the spatial flux is concentrated between the range of 500 ± 5 km, 225 ± 5 kg. The overall distribution is where the maximum value becomes $9.212 \times 10^{-5}/\mathrm{m}^2/\mathrm{yr}$ at 499.5452 km, 222.6219, and the latter value becomes 757.56 times the former value; the flux change of CORVUS BC5 is more concentrated compared with the flux change of GAOFEN. This change has some relationship with the volume of both, and the overall change trend is similar to that of Alt-V. The effect of the different characteristics of the satellites is similar between the different types of fluxes.

Figure 6e,f shows the comparison of Alt-Mass flux variation of YAOGAN-35C satellite. Before considering Starlink, the spatial flux of YAOGAN-35C is concentrated in the range of 475–520 km, below 50 kg. The size is relatively average and there is no extremely high value. The maximum value is 521.7986 km, 0.67962 kg at $2.914 \times 10^{-8}/\mathrm{m}^2/\mathrm{yr}$; this situation is similar to the distribution of Alt-V. After considering Starlink, the spatial flux distribution

becomes concentrated, mainly in the range of 482–510 km, 210–230 kg, and the maximum value is higher and varies greatly. The maximum value becomes 504.2253 km, 222.6219 kg at 4.257 $\times$ 10^{-5}/m^2/yr, 1460.878 times that of the former, considering the influence of Starlink before and after on the flux variation. Similar variation trends for Alt-V and Alt-Mass indicate that there is a difference in the influence of different satellite characteristics on the satellite flux variation and that the flux variation caused by the change in inclination angle is distinct from the flux variation caused by the change in volume and mass. The effect of inclination angle on flux is more significant, and it also demonstrates that the effect of Starlink inclusion on flux variation of LEO satellites is evident. Some satellites with more special characteristics are more dangerous in this situation, implying that the choice of some mission orbits becomes more dangerous in the face of the complex LEO space situation, and there even be a situation where the orbit is no longer viable.

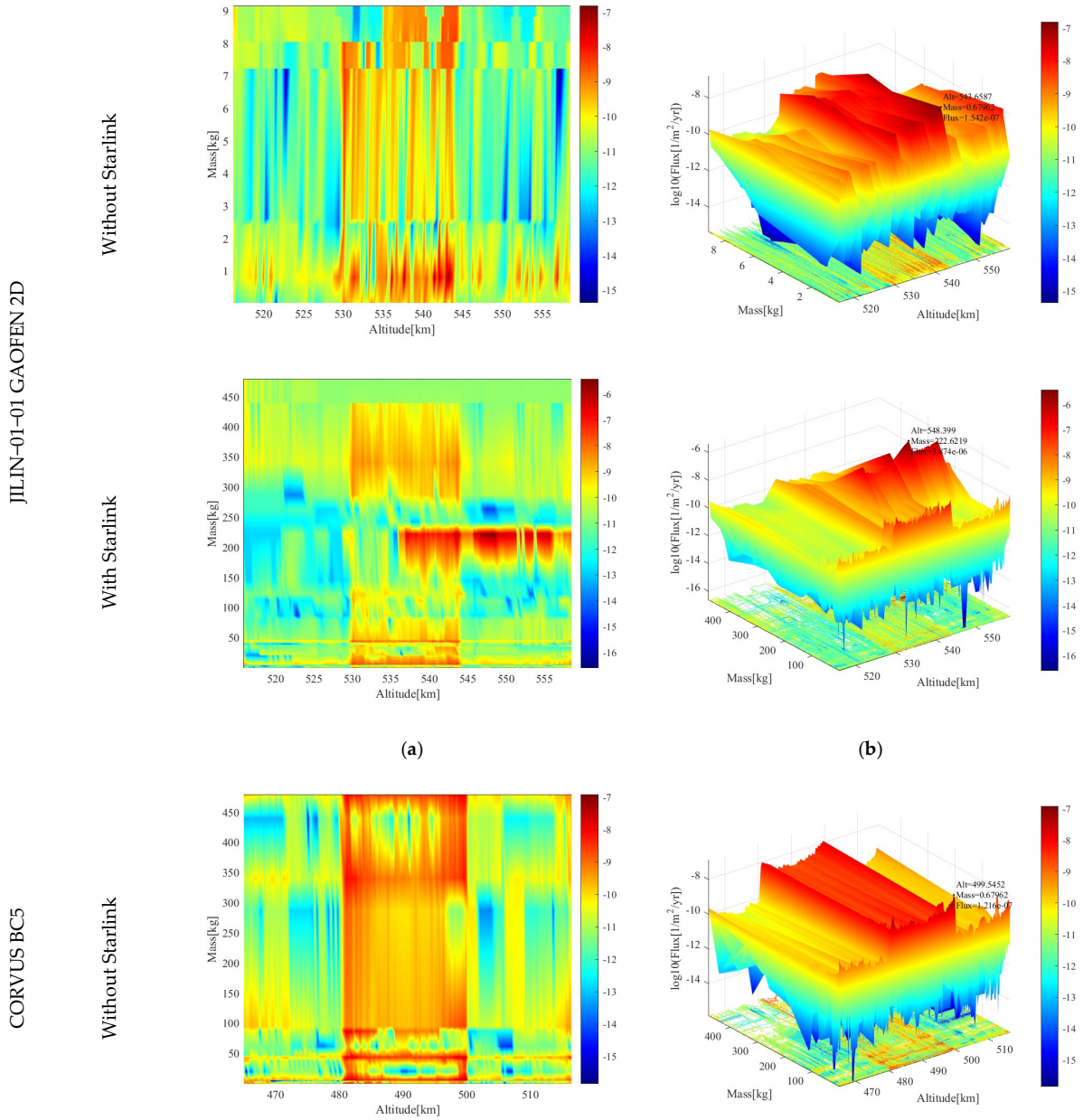

Figure 6. *Cont.*

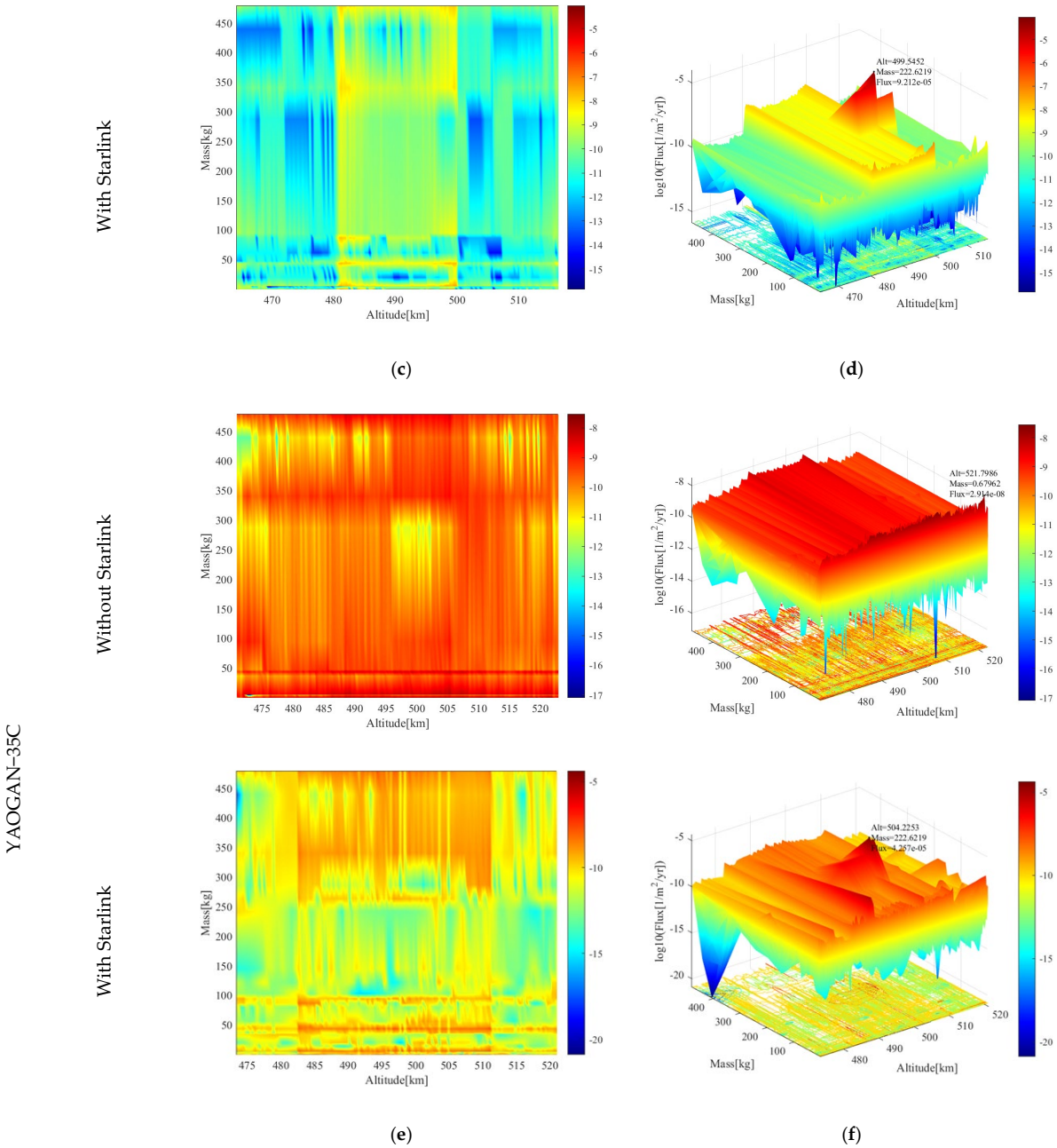

Figure 6. Object height fluxes and object size fluxes. (**a**,**b**) Before and after Alt-Mass fluxes of GAOFEN satellites; (**c**,**d**) Before and after Alt- Mass fluxes of CORVUS BC5 satellites; (**e**,**f**) Before and after Alt- Mass fluxes of YAOGAN-35C satellites.

The Starlink constellation has a significant impact on the Earth's low orbit environment from a flux perspective. To exclude the unique characteristics of the satellites themselves, which would render the results unreliable, three target satellites with distinct characteristics were chosen for analysis and calculation. Mass and Alt-V flux variation data allowed us to calculate the ACPL values of the three target satellites and the corresponding number of avoidance operations. The specific data are provided below. It should be noted that, despite the drastic flux variation, the impact of flux variation on a target satellite's collision probability may be different due to the target satellite's volume and mass, and this difference will be reflected in the impact on its ACPL.

4. Impact of Starlink on Control Avoidance Strategies for low-orbiting Satellites in Geospace

4.1. Impact on ACPL Values for LEO Space Target Satellites

According to the flux, we can get the ACPL value of the target satellite with its corresponding average daily manipulation frequency, risk variation curve, etc. The manipulation frequency and risk (collision probability) corresponding to different ACPL values are shown in Figure 7. Risk Reduction is the risk that decreases with the number of manipulations, and Residual Risk is the risk that remains. In the following analysis, only the variation of risk of known objects is discussed. For ACPL, 10^{-4} is a more acceptable value at present [15], attributed to its balance of safety as well as economy. ACPL-10^{-6} is added for comparison to reflect the nature of the value.

In Figure 7a,b when Starlink is not considered, the ACPL value chosen for 10^{-6} corresponds to a manipulation frequency of 0.201, 10^{-4} to 0.036, and a risk of 2.27×10^{-6}.

After adding Starlink, the manipulation frequency corresponding to ACPL-10^{-6} is 1.24, the manipulation frequency corresponding to ACPL-10^{-4} is 0.0811, and the risk is 1.27×10^{-5}, which reaches the yellow warning threshold. Before and after changes, the manipulation frequency of ACPL-10^{-4} becomes 2.252 times that of the previous one, and the risk of known objects becomes 5.5947 times that of the previous one. Considering Starlink before and after the change, ACPL-10^{-6} operates 5.58 and 15.28 times more frequently compared to ACPL-10^{-4}, which reflects the more reasonable choice of ACPL-10^{-4} from the side.

The addition of Starlink to Earth's low-orbit space has not reduced any risk, even though the frequency of operations has changed several times, indicating that the overall risk is greater than before, i.e., Starlink has introduced harsher changes to the Earth's space environment and it would be difficult to alter the current environmental conditions within the range of conventional changes.

Figure 7c,d shows the ACPL value of CORVUS BC5 versus the manipulation frequency and risk, with the manipulation frequency of 1.76 for ACPL-10^{-6}, 0.0834 for ACPL-10^{-4} and 1.22×10^{-5} when Starlink is not added.

After adding Starlink, the manipulation frequency of ACPL-10^{-6} becomes 6.73, the manipulation frequency corresponding to ACPL-10^{-4} is 1.16, and the risk is 5.4×10^{-5}. In comparison of the situations before and after change, the manipulation frequency corresponding to ACPL-10^{-6} changes to 3.823 times of the previous one; the risk of known objects does not change; the manipulation frequency of ACPL-10^{-4} becomes 13.9 times of the previous one, and the risk of known objects becomes 4.5 times of the previous one. While taking Starlink into consideration, the manipulation frequency of ACPL-10^{-6} compared to ACPL-10^{-4} is 21.103 and 5.80 times of the previous one, respectively. The overall change pattern of CORVUS BC5 is similar to GAFEN.

Figure 7e,f shows the relationship between the ACPL value of YAOGAN-35C and the manipulation frequency and risk; without Starlink, the manipulation frequency of ACPL-10^{-6} is 0.334, the manipulation frequency corresponding to ACPL-10^{-4} is 0.0809, and the risk is 2.63×10^{-6}.

After adding Starlink, the manipulation frequency of ACPL-10^{-6} becomes 12.7, the corresponding manipulation frequency of ACPL-10^{-4} is 1.68, and the risk is 1.65×10^{-4}, which has exceeded the yellow warning threshold. The manipulation frequency of ACPL-10^{-4} becomes 20.76 times of the previous one, and the risk of known objects becomes 62.73 times that of the previous one before and after changes; considering Starlink before and after, the manipulation frequency of ACPL-10^{-6} compared to ACPL-10^{-4} is 4.12 and 7.55 times more frequent than before, respectively. Combining the three comparison groups, from the Figure 7 overall results, the impact of Starlink on target satellites in geospace is extremely significant, and the choice of ACPL-10^{-4} is more reasonable than ACPL-10^{-6} in terms of both economic and safety considerations.

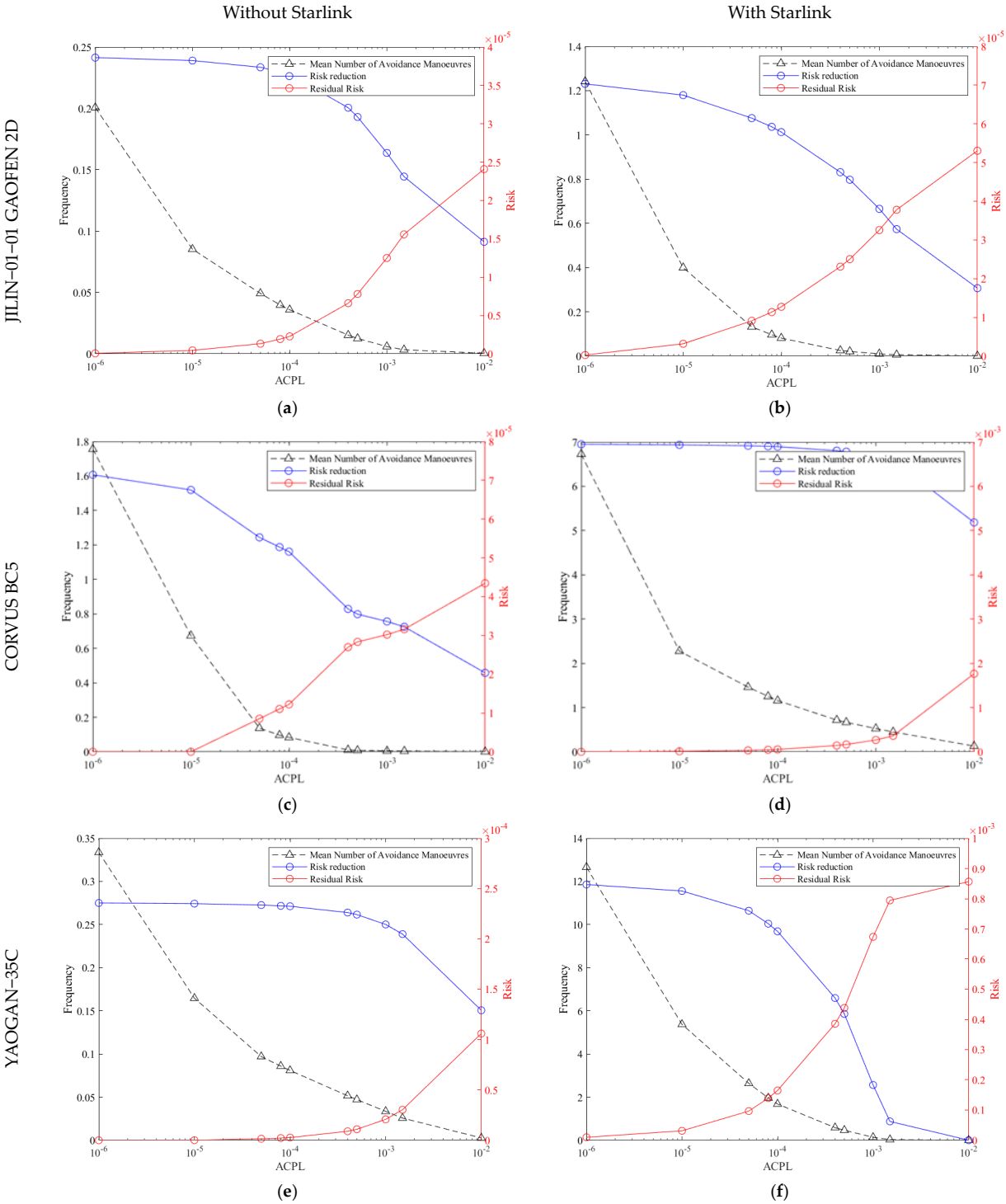

Figure 7. Comparison of ACPL values and average maneuvering coefficients for satellites with and without Starlink constellation. (**a**,**b**) The variation of GAOFEN satellites in the frequency and risk to different ACPL values With Starlink and Without Starlink; (**c**,**d**) The variation of CORVUS BC5 satellites in the frequency and risk to different ACPL values With Starlink and Without Starlink; (**e**,**f**) The variation of YAOGAN-35C satellites in the frequency and risk to different ACPL values With Starlink and Without Starlink.

Considering Starlink before and after the change, ACPL-10^{-4} corresponding to the operating frequency of the three target satellites in the minimum operating frequency change has doubled, and it can be clearly observed that joining Starlink to choose ACPL-10^{-6}

would render the risk at 0. However, as the frequency of control avoidance increases significantly, it is evident that it can not be adhered to over the long term, which means that, considering the issue of mission life, the target satellite must select a more reasonable ACPL value. However, even if the number of orbital avoidance controls vastly exceeds the number before Starlink is considered, the geospace environment will worsen. Even with the most aggressive orbital avoidance controls, the deterioration of the geospace environment is an irreversible and deteriorating process.

Avoidance of controls reduces risk, and the risk relationship corresponding to the frequency of manipulation is shown in Figure 8. The Fractional Residual Risk in the figure represents the residual partial risk coefficient that varies according to the number of manipulations and is used only as a quantity to describe the degree of risk and not as a specific numerical reference. The relationship between the change in risk level and the change in the number of maneuvers can be observed visually in the graph. In order to observe the relationship and pattern of different maneuvering frequencies before and after each consideration of Starlink, the maneuvering frequencies corresponding to different ACPL values were selected in the three target satellites for comparison. In the following, risk coefficient indicates the degree of presence of risk, with a maximum value of 1. Risk indicates the probability of collision.

In Figure 8a,b the risk coefficient for a manipulation frequency of 0.201 without Starlink is 1.68×10^{-3} and the risk is 6.5×10^{-8}, and the risk coefficient for a manipulation frequency of 1.24 with Starlink is 3.58×10^{-3} and the risk is 2.52×10^{-7}. It is obviously observed that the risk coefficient increases by 2.13 times when the manipulation frequency reaches the maximum in both comparison groups. The coefficient of risk is 2.13-times greater after considering Starlink when the manipulation frequency is 6.16-times greater than before, indicating that the coefficient of risk inevitably rises after considering Starlink, even if the manipulation frequency is doubled.

In Figure 8c,d when the manipulation frequency is the smallest in the two comparison groups, the corresponding risk coefficient is 0.681 with a risk of 4.35×10^{-5} when the manipulation frequency is 6.88×10^{-4} without considering Starlink, and the corresponding risk coefficient is 0.254 with a risk of 1.73×10^{-3} when the manipulation frequency is 0.131 when considering Starlink. Furthermore, the corresponding risk coefficient is 0.372 when the manipulation frequency is 190.4-times of the previous one in the two comparison groups. Manipulation frequency at the minimum, the risk coefficient becomes 0.372-times after the manipulation frequency becomes 190.4-times the previous one, and this comparison group data shows that when the manipulation frequency increases across orders of magnitude, its corresponding risk coefficient can be reduced compared to the previous one, but the effect is weaker and not proportional to the growth of the manipulation frequency, i.e., the consumption is too great for half the effort.

In Figure 8e,f we choose a more moderate manipulation frequency, i.e., the manipulation frequency corresponding to ACPL-10^{-4}. The risk coefficient corresponding to a manipulation frequency of 0.0809 is 0.0112 with a risk of 2.63×10^{-6} when Starlink is not considered. The risk coefficient corresponding to a manipulation frequency of 1.68 is 0.192 with a risk of 1.65×10^{-4} when Starlink is considered. With 1.65×10^{-4}, the risk coefficient becomes 17.143-times greater after the manipulation frequency becomes 20.77-times greater than the previous one, a data set that corroborates the fact that the corresponding risk coefficient still grows with a similar multiplication when the manipulation frequency grows insignificantly.

One thing the above data show is that increasing operating frequency after taking Starlink into account does not guarantee that the risk coefficient decreases or even returns to the original tier; in the case where the increase in operating frequency is not of a large order of magnitude, the risk coefficient is even larger than before, indicating that the overall risk magnitude increases, and the residual risk is operated even if it is 10% of the original risk. It is further exhibited that even if the number of orbit avoidance controls is significantly higher than before Starlink is considered, it will still face a worse geospace environment.

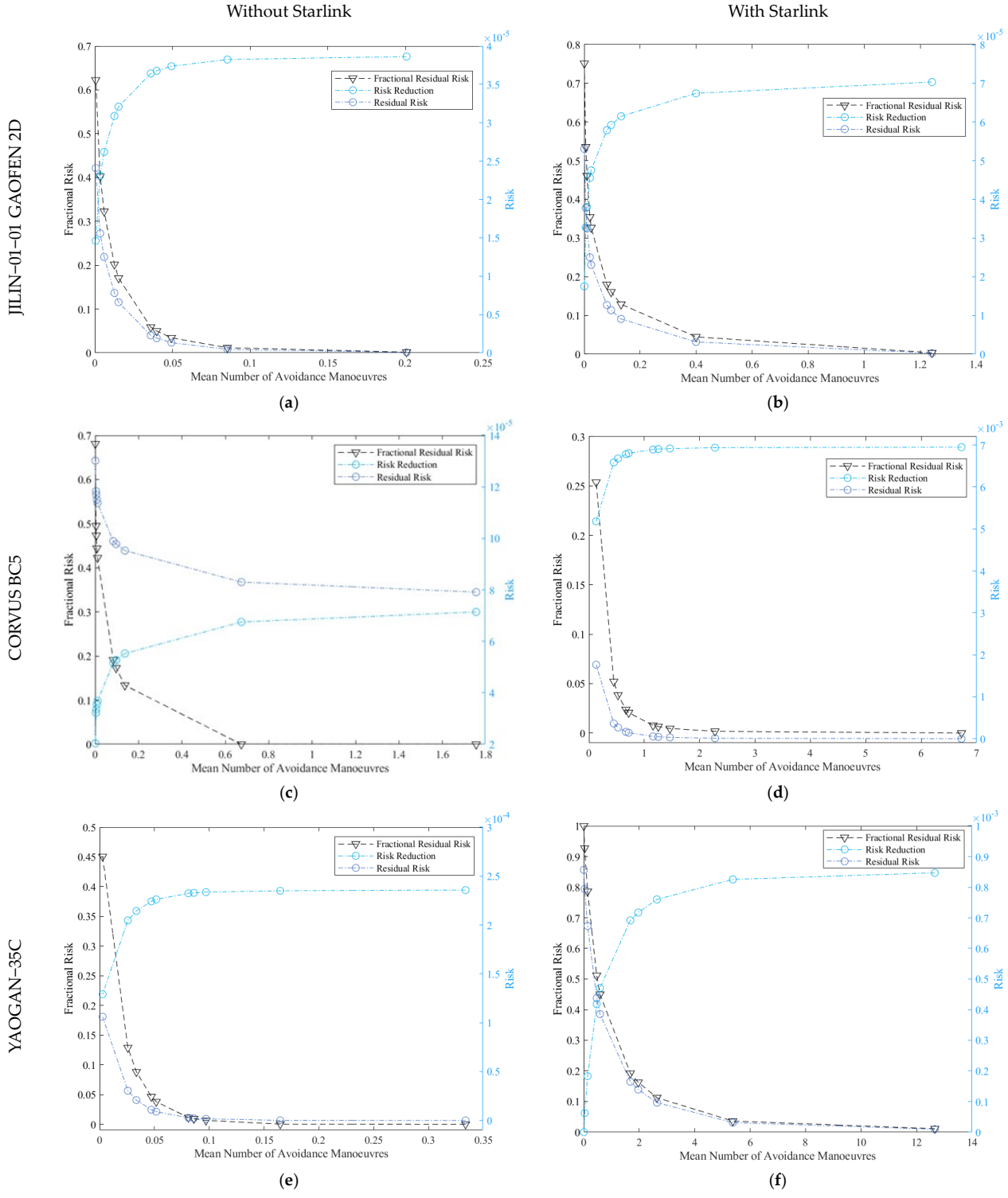

Figure 8. Average number of operations vs. residual risk. (**a**,**b**) The variation of GAOFEN satellites in fractional risk and risk to different Mean Number of Avoidance Manoeuvres With Starlink and Without Starlink; (**c**,**d**) The variation of CORVUS BC5 satellites in fractional risk and risk to different Mean Number of Avoidance Manoeuvres With Starlink and Without Starlink; (**e**,**f**)The variation of YAOGAN-35C satellites in fractional risk and risk to different Mean Number of Avoidance Manoeuvres With Starlink and Without Starlink.

From the preceding discussions, it can be deduced that Starlink has an impact on the target satellites due to the large number of satellites dispersed across their entire orbit, and that the degree of impact corresponds to the degree of flux variation.

When ACPL-10^{-4} is selected, when comparing to the case without Starlink, the avoidance frequency of GAOFEN satellites increases by a factor of 2.252, and the collision risk with or without Starlink is 2.27 $\times$ 10^{-6} and 1.27 $\times$ 10^{-5} respectively. However, the risk increases to 5.5947-times greater than the previous one.

CORVUS BC5 with its ACPL-10^{-4} has increased its avoidance frequency by a factor of 13.9, with a collision risk of 1.22 $\times$ 10^{-5} and 5.4 $\times$ 10^{-5}, respectively. While changing the risk to 4.5-times greater than the previous one, while maintaining the ACPL-10^{-4}, indicating an increased avoidance frequency. However, again the risk is shown to increase rather than decrease.

YAOGAN-35C's ACPL value of 10^{-4} increases the frequency of avoidance control by about 20.76 times, and the collision risk is 2.63 $\times$ 10^{-6} and 1.65 $\times$ 10^{-4}, respectively, becoming 62.73-times higher before Starlink is considered.

In Figure 8, the relationship between the frequency of control avoidance and its corresponding risk coefficient and risk, the following conclusion can be drawn: after considering Starlink, the growth of the operation frequency does not guarantee that the risk coefficient decreases or even returns to the original tier, and the growth of the operation frequency is even accompanied by the growth of the risk coefficient in the case that the growth of the operation frequency is not of a large order of magnitude.

4.2. Impact on LEO Space Target Satellite Deorbit Capability

In order to refine the impact of Starlink on the target satellite in terms of risk and avoidance operations, this section presents the changes in ΔV and propellant mass fraction (PMF) required before and after considering Starlink for different ACPL values. The effects of early and temporary Orbital maneuvering on these values are also indicated.

The ΔV required for the three target satellites to avoid control is depicted in Figure 9, which shows the earliest ΔV from 10 revolutions ago to avoid control in advance. In order to summarize the data in more comprehensive detail, the data in Figure 9 are summarized in Table 4, and the more concerned information is extracted from the figure for visual comparison. There, 0Revs/10Revs indicates the ratio of ΔV consumed at 0 Revolutions to that consumed at 10 Revolutions. Also, With Starlink ACPL/Without Starlink ACPL indicate the ratio of ΔV consumed with and without Starlink.

In Figure 9a,b a smaller ACPL value requires a larger ΔV value to be satisfied, and the ΔV of ACPL-10^{-6} and ACPL-10^{-4} without advance avoidance control is 9.08- and 4.837-times that of avoidance control with 10 revolutions in advance. ACPL-10^{-6} and ACPL-10^{-4} without early avoidance control are 7.16- and 5.837-times those with 10 revolutions of early avoidance control. Without early avoidance control, ACPL-10^{-6}-ΔV and ACPL-10^{-4}-ΔV are 3.98- and 2.27-times of those with Starlink, respectively, and ACPL-10^{-6}-ΔV and ACPL-10^{-4}-ΔV with 10 revolutions of early avoidance control are 3.98- and 2.27-times of those with Starlink. ACPL-10^{-6}-ΔV and ACPL-10^{-4}-ΔV are 5.05- and 1.88-times the considered ones, respectively.

In Figure 9c,d the difference with Figure 9a,b is the change in order of magnitude. After considering Starlink, the ΔV surge, without advance avoidance control, ACPL-10^{-6}-ΔV becomes 82.822 times before considering Starlink, ACPL-10^{-4}-ΔV becomes 556.129 times, and with advance avoidance control, ACPL-10^{-6}-ΔV becomes 56.944 times before considering Starlink, ACPL-10^{-4}-ΔV becomes 332.733 times. At 10 revolutions of avoidance control, ACPL-10^{-6}-ΔV becomes 56.944 times and ACPL-10^{-4}-ΔV becomes 332.733 times before Starlink is considered, and the effect of Starlink on CORVUS BC5 is more severe, which is consistent with the flux changes reflected in Section 3. In the case of avoidance control by considering Starlink, a greater change in ΔV is required for early avoidance control than for immediate avoidance control, for example, the ΔV ratio is 26.050 for both without Starlink, 43.535 with Starlink considered, and 9.055 and 13.170 with ACPL-10^{-4}, respectively.

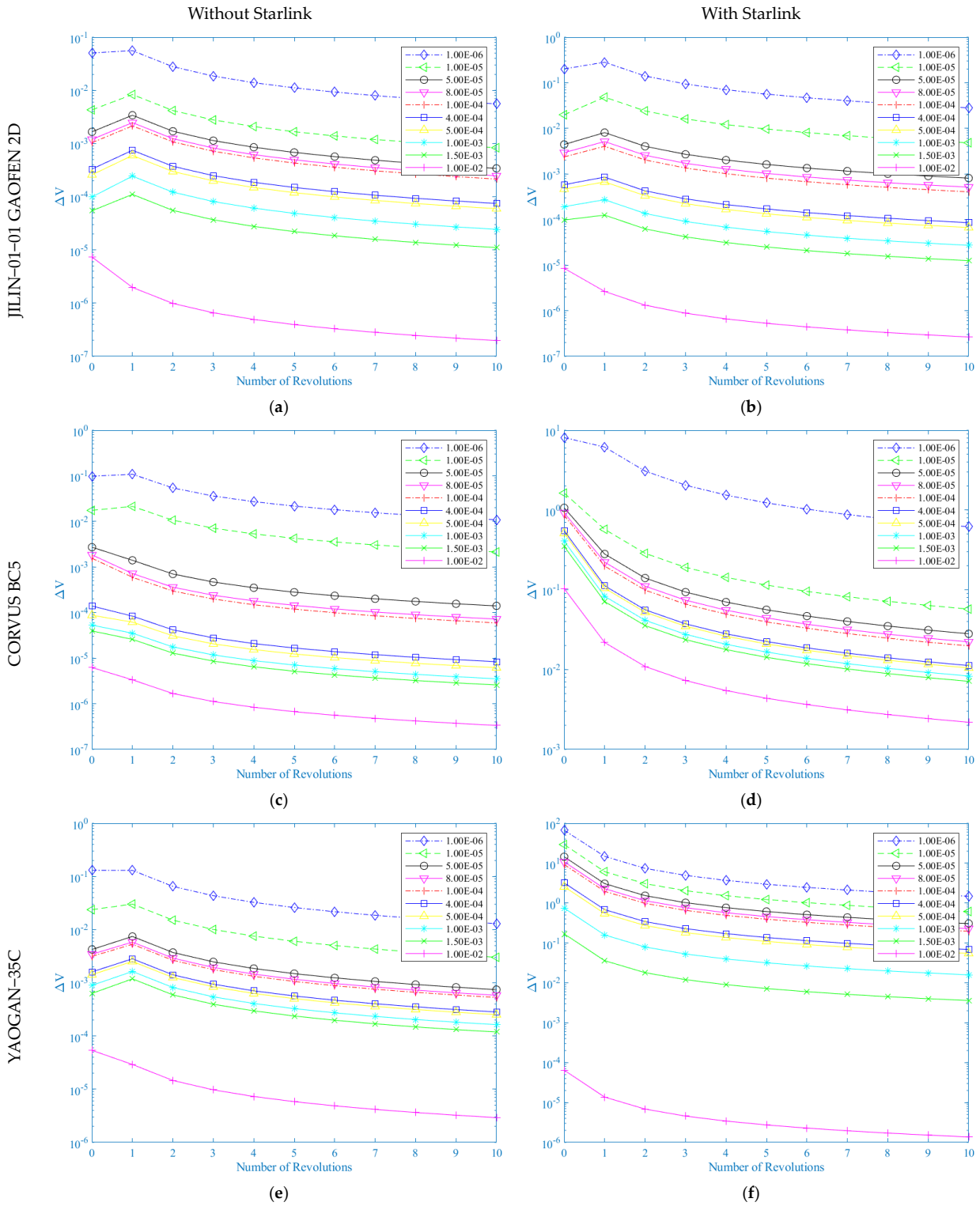

Figure 9. Required for different ACPL values in ten revolutions to change track ΔV.(**a**,**b**) Comparison of different ΔV variations with and without Starlink for GAOFEN; (**c**,**d**) Comparison of different ΔV variations with and without Starlink for CORVUS BC5; (**e**,**f**) Comparison of different ΔV variations with and without Starlink for YAOGAN-.

Table 4. Comparison of data from ΔV in Figure 9.

Name	Revolutions		0	5	10	$\frac{\text{0 Revs}}{\text{10 Revs}}$
JILIN-01-01 GAOFEN 2D	*Without Starlink*	ACPL-10^{-6}	5.07×10^{-2}	1.12×10^{-2}	5.58×10^{-3}	9.08
	With Starlink	ACPL-10^{-6}	2.02×10^{-1}	5.64×10^{-2}	2.82×10^{-2}	7.16
	$\frac{\text{With Starlink ACPL}}{\text{Without Starlink ACPL}}$		3.984	5.035	5.053	
	Without Starlink	ACPL-10^{-4}	1.04×10^{-3}	4.30×10^{-4}	2.15×10^{-4}	4.837
	With Starlink	ACPL-10^{-4}	2.37×10^{-3}	8.11×10^{-4}	4.06×10^{-4}	5.837
	$\frac{\text{With Starlink ACPL}}{\text{Without Starlink ACPL}}$		2.278	1.886	1.888	
CORVUS BC5	*Without Starlink*	ACPL-10^{-6}	9.78×10^{-2}	2.17×10^{-2}	1.08×10^{-2}	9.055
	With Starlink	ACPL-10^{-6}	8.10	1.23	6.15×10^{-1}	13.170
	$\frac{\text{With Starlink ACPL}}{\text{Without Starlink ACPL}}$		82.822	56.682	56.944	
	Without Starlink	ACPL-10^{-4}	1.55×10^{-3}	1.19×10^{-4}	5.95×10^{-5}	26.050
	With Starlink	ACPL-10^{-4}	8.62×10^{-1}	3.96×10^{-2}	1.98×10^{-2}	43.535
	$\frac{\text{With Starlink ACPL}}{\text{Without Starlink ACPL}}$		556.129	332.773	332.773	
YAOGAN-35C	*Without Starlink*	ACPL-10^{-6}	1.31×10^{-1}	2.61×10^{-2}	1.30×10^{-2}	10.076
	With Starlink	ACPL-10^{-6}	6.68×10^{1}	2.96	1.48	45.135
	$\frac{\text{With Starlink ACPL}}{\text{Without Starlink ACPL}}$		509.923	113.409	113.846	
	Without Starlink	ACPL-10^{-4}	3.15×10^{-3}	1.06×10^{-3}	5.31×10^{-4}	5.932
	With Starlink	ACPL-10^{-4}	9.24	3.93×10^{-1}	1.97×10^{-1}	46.903
	$\frac{\text{With Starlink ACPL}}{\text{Without Starlink ACPL}}$		2933.33	370.75	370.998	

Figure 9e,f shows a pattern similar to that of Figure 9c,d. Figure 9 reflects a general pattern in which ΔV without advance control avoidance is much larger than that without Starlink, which only occurs in CORVUS BC5 and YAOGAN-35C, and YAOGAN -35C is much better than CORVUS BC5.

According to the characteristics of the three target satellites, when only the three factors of altitude, inclination, and area are considered, the orbit altitude has a greater impact on the avoidance operation, the target satellite's area has a greater impact, and inclination has a minor impact. Early orbital maneuvering is advantageous in the avoidance operation because it reduces the orbital maneuvering consumption of various types of target satellites. The increase in the frequency of avoidance operation after considering Starlink brings the increase of ΔV, and the change of ΔV supports the huge avoidance consumption of target satellites after considering Starlink from the level of results. Starlink has a huge impact on the target satellite.

What is more intuitive than the speed required for orbital maneuvering is the propellant required for orbital maneuvering. The change of speed requires propellant, because the three target satellites have different orbital maneuvering methods and different satellite

masses, so in order to compare the propellant consumption more intuitively, the propellant mass fraction is used to show the propellant consumption. In Figure 10, the propellant mass fraction (PMF) required by the target satellite before and after Starlink is considered and the effect of early orbital maneuvering on PMF are shown. It can be observed from Table 5 that the trend of PMF is basically consistent with ΔV. PMF expresses the ratio of consumed propellant to satellite mass, which is defined as shown in Equation (5), $M_{prop-per}$ represents the consumed propellant mass, M_{sat} represents the satellite mass, and $M_{prop-all}$ represents all propellant masses.

$$PMF = \frac{M_{prop-per}}{M_{prop-all} + M_{sat}} \tag{5}$$

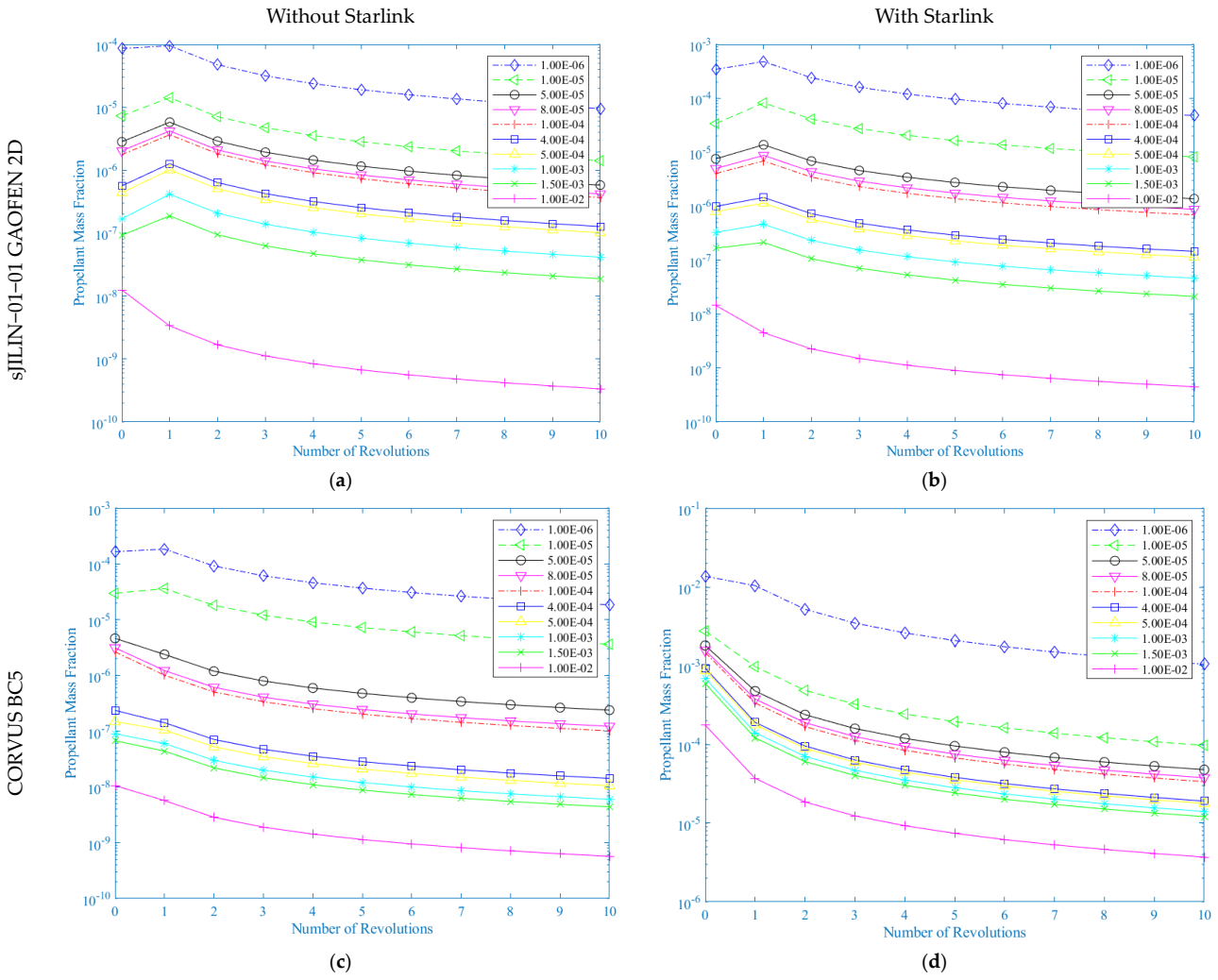

Figure 10. *Cont.*

YAOGAN−35C

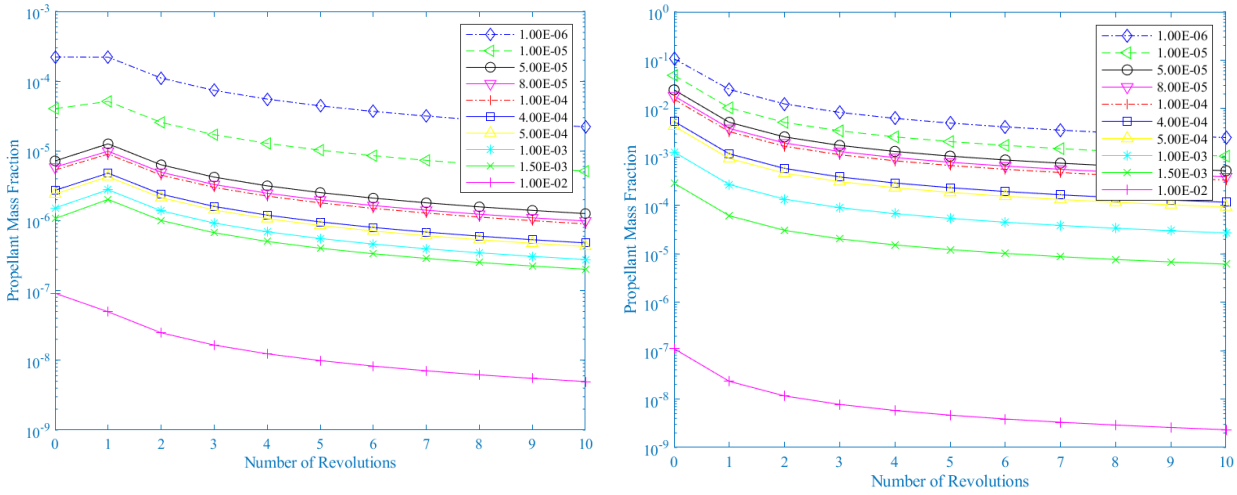

Figure 10. Propellant coefficients required for orbit change at different ACPL values during the revolution. (**a**,**b**) Comparison of different PMF variations with and without Starlink for GAOFEN; (**c**,**d**) Comparison of different PMF variations with and without Starlink for CORVUS BC5; (**e**,**f**) Comparison of different PMF variations with and without Starlink for YAOGAN-35C.

For most satellites the probability of problems with the payload itself is extremely low, so the life of a satellite is designed to be measured in terms of propellant, and when the propellant is depleted, the life of a satellite is over. Orbital avoidance consumes propellant, and when satellites change orbit more often due to excessive avoidance, the lifetime of the satellite is affected [30,31].Assuming a lifetime of 5 years for one satellite in the case of ACPL-10^{-4} when Starlink is not considered, the lifetime of the three satellites is shortened by 56.21%, 99.09%, and 99.82% when Starlink is considered without advance avoidance control; the lifetime of the three satellites is shortened by 10 revolutions of advance avoidance control without Starlink, when assuming that each warning event satellite can be detected in the case of avoiding control 10 revolutions in advance, without considering Starlink. Assuming that each warning event satellite can be detected and controlled in advance, the lifetime of the three target satellites can be extended by 380%, 502.6%, 493.12%. However, when considering Starlink, the lifetime of GAOEN is extended by 155.44%, and the other two target satellites are shortened by 92.166%, 91.99%, respectively. The data shows that the target satellites with orbital altitude around 500 km are more susceptible to Starlink's interference, while the inclination angle has little effect.

Avoidance consumes propellant, but as previously stated, the same amount of propellant consumption does not achieve the same avoidance effect, and using more propellant to achieve the same ACPL value does not achieve the same level of risk. This effect can be reduced to a minimum if avoidance is carried out in advance. However, how to provide early warning of collision timing, which requires accurate orbit forecasting, is a challenge. The purpose of this paper is to assess the risk of future collision and its repercussions for the satellite's avoidance strategy. The objective of the paper is to assess the impact of future collision risk on the satellite avoidance strategy, and the findings are not encouraging. Because of the emergence of mega constellations, target satellites of all types are affected, and this impact is comprehensive, affecting not only the satellite's safety but also depleting the satellite's in−orbit lifetime; frequent avoidance will result in the satellite's premature loss of power and abandonment.

Table 5. Comparison of PMF data in Figure 9.

Name	Revolutions		0	5	10	$\frac{\text{0 Revs}}{\text{10 Revs}}$
JILIN-01-01 GAOFEN 2D	*Without Starlink*	ACPL-10^{-6}	8.61×10^{-5}	1.90×10^{-5}	9.49×10^{-6}	9.072
	With Starlink	ACPL-10^{-6}	3.44×10^{-4}	9.59×10^{-5}	4.79×10^{-5}	7.18
	$\frac{\text{With Starlink ACPL}}{\text{Without Starlink ACPL}}$		3.995	5.047	5.047	
	Without Starlink	ACPL-10^{-4}	1.76×10^{-6}	7.32×10^{-7}	3.66×10^{-7}	4.808
	With Starlink	ACPL-10^{-4}	4.02×10^{-6}	1.38×10^{-6}	6.89×10^{-7}	5.834
	$\frac{\text{With Starlink ACPL}}{\text{Without Starlink ACPL}}$		2.284	1.885	1.882	
CORVUS BC5	*Without Starlink*	ACPL-10^{-6}	1.66×10^{-4}	3.68×10^{-5}	1.84×10^{-5}	9.021
	With Starlink	ACPL-10^{-6}	1.37×10^{-2}	2.09×10^{-3}	1.05×10^{-3}	13.047
	$\frac{\text{With Starlink ACPL}}{\text{Without Starlink ACPL}}$		82.530	56.793	57.065	
	Without Starlink	ACPL-10^{-4}	2.64×10^{-6}	2.02×10^{-7}	1.01×10^{-7}	26.138
	With Starlink	ACPL-10^{-4}	1.46×10^{-3}	6.73×10^{-5}	3.37×10^{-5}	43.323
	$\frac{\text{With Starlink ACPL}}{\text{Without Starlink ACPL}}$		5563.030	333.168	333.663	
YAOGAN-35C	*Without Starlink*	ACPL-10^{-6}	2.22×10^{-4}	4.43×10^{-5}	2.21×10^{-5}	10.045
	With Starlink	ACPL-10^{-6}	1.07×10^{-1}	5.02×10^{-3}	2.51×10^{-3}	42.629
	$\frac{\text{With Starlink ACPL}}{\text{Without Starlink ACPL}}$		481.981	113.318	113.574	
	Without Starlink	ACPL-10^{-4}	5.35×10^{-6}	1.80×10^{-6}	9.02×10^{-7}	5.931
	With Starlink	ACPL-10^{-4}	1.56×10^{-2}	6.68×10^{-4}	3.34×10^{-4}	46.706
	$\frac{\text{With Starlink ACPL}}{\text{Without Starlink ACPL}}$		2915.887	371.111	370.288	

5. Discussion and Conclusions

The collision probability of the Starlink constellation with the target satellite was calculated in this paper by calculating its various altitude and mass object fluxes to LEO satellites, and the collision probability was evaluated by the ARES module of DRAMA to obtain the satellite's ACPL value, as well as the corresponding maneuver frequency, risk level, and control avoidance consumption. This study sought to determine the impact of the mega constellation on the control avoidance strategy of the target satellite. The following conclusions were obtained.

(1) The target satellites with varying ranges of area, orbital altitude, and inclination are significantly impacted by Starlink, indicating that Starlink has a comprehensive effect on LEO satellites. However, these three characteristics also vary in the degree to which Starlink affects the target satellites, with orbital altitude having the greatest impact, followed by inclination and area.

(2) In the case of ACPL-10^{-4}, the manipulation frequency of the three target satellites becomes 2.252, 13.9, and 20.76 times that of the previous one when Starlink is considered, and the change trend is similar to the flux. For the same ACPL values, the risks of the

three have increased, becoming 5.5947, 4.5, and 62.73 times more than the previous ones, which means that even with frequent control avoidance, the geospace environment does not improve, i.e., the total amount of risk becomes greater, the same proportional residual risk becomes higher, and therefore the same ACPL values require more control avoidance maneuvers after the influence of Starlink. However, even if the same ACPL value is reached, the collision risk latter is much higher than the former; even with more propellant consumed, the risk present is still not effectively removed. Furthermore, corroborating this argument is the change of the maneuvering frequency with its corresponding risk coefficient, where the maneuvering frequency becomes 6.16, 190.4, 20.77 times greater than the previous one, which respectively becomes 2.13, 0.372, and 17.143 times greater than the previous one. The increase in manipulation frequency after considering Starlink does not guarantee that the risk coefficient decreases or even returns to its original tier, and the increase in manipulation frequency is even accompanied by an increase in the risk coefficient in cases where the increase in manipulation frequency is not of a large order of magnitude.

(3) The effect of the change of ΔV on the orbital maneuver of the target satellite and the effect of early orbital maneuver on ΔV are initially obtained from the change. According to the characteristics of the three target satellites, the orbital altitude has a greater effect on the avoidance control, and the area of the target satellite plays a greater effect. The inclination angle, on the other hand, does not play a significant role. In the avoidance operation, the early orbital maneuvering is beneficial to reduce the orbital maneuvering consumption of different types of target satellites. The increase in frequency of avoidance operation after considering Starlink results in the increase of ΔV, and the change of ΔV supports the huge avoidance consumption of target satellites after considering Starlink from the level of result. Starlink has a huge impact on the target satellite.

(4) When avoidance is not performed in advance, the lifetime of the three satellites is shortened by 56.21%, 99.09%, and 99.82% after taking Starlink into account, and when avoidance is performed in advance, the lifetime of the three satellites is shortened by 10 revolutions without taking Starlink into account, assuming that the satellites can detect and avoid each warning event in advance. The lifetimes of the three target satellites can be extended by 380%, 502.6%, and 493.12%, respectively, but in the case of Starlink, the lifetime of the other two target satellites is extended by 155.44%, and the lifetimes of other two target satellites are shortened by 92.166%, 91.99%, respectively, according to the characteristics of the three target satellites combined with the data. According to the characteristics of the three target satellites and the data, the orbital altitudes of the target satellites change more after being affected by Starlink, so the effects of Starlink should be considered more thoroughly for some satellites with orbital altitudes in specific areas.

We can see from the calculated values that taking Starlink into account makes the geospace environment of the three target satellites harsher, but some features cause a bigger impact than others. Of the three features considered in this paper, orbital altitude constitutes the biggest impact, followed by area and inclination. According to the findings, increasing the frequency of avoidance control after considering Starlink does not improve the risk situation, the results from avoidance control do not improve, and the deterioration of the geospace environment is irreversible. Given an orbital altitude higher than YAOGAN-35C, CORVUS BC5, and in advance, Starlink has significantly less effect on JILIN-01 GAOFEN 2D. Given early avoidance control, Starlink is guaranteed to not result in any impact on its mission lifetime, but for the first two, even with early avoidance control, less than 10 percent of the mission lifetime remains.

Author Contributions: Conceptualization, H.T., X.L., Q.Z. and X.C.; methodology, H.T. and X.C.; software, H.T.; validation, H.T., W.M., Z.Z. and G.Z.; formal analysis, H.T.; investigation, H.T.; resources, X.L., Q.Z. and X.C.; writing—original draft preparation, H.T.; writing—review and editing, H.T. and X.C.; visualization, H.T.; supervision, X.L. and Q.Z.; All authors have read and agreed to the published version of the manuscript.

Funding: This research received no external funding.

Data Availability Statement: Not Applicable.

Acknowledgments: The authors wish to thank the anonymous reviewers for their valuable suggestions.

Conflicts of Interest: The authors declare no conflict of interest.

References

1. Weimer, B.D. Application for Fixed Satellite Service by WorldVu Satellites Limited, Debtor-in-Possession [SAT-MPL-20200526-00062]. Available online: https://fcc.report/IBFS/SAT-MPL-20200526-00062 (accessed on 23 December 2021).
2. Foust, J. FCC Approves Starlink License Modification. Available online: https://spacenews.com/fcc-approves-starlink-license-modification/ (accessed on 28 December 2021).
3. E-Space. Available online: https://www.E-Space.com/news/E-Space-to-launch-demonstration-satellites-in-q2-with-rocket-lab (accessed on 19 July 2022).
4. ITU: Committed to Connecting the World. Available online: https://www.itu.int/en/Pages/default.aspx (accessed on 30 May 2022).
5. Hindin, J.D. Application for Fixed Satellite Service by Kuiper Systems LLC [SAT-LOA-20190704-00057]. Available online: https://fcc.report/IBFS/SAT-LOA-20190704-00057 (accessed on 21 June 2022).
6. Hainaut, O.R.; Williams, A.P. Impact of satellite constellations on astronomical observations with ESO telescopes in the visible and infrared domains. *Astron. Astrophys.* **2020**, *636*, A121. [CrossRef]
7. Oltrogge, S.D.L. Alfano Collision Risk in Low Earth Orbit. In Proceedings of the International Astronautical Congress 2016, Paper IAC-16-A6,2,1,x32763. Guadalajara, Mexico, 26–30 September 2016.
8. WIltshire, W. Application for Fixed Satellite Service by Space Exploration Holdings, LLC [SAT-MOD-20200417-00037]. Available online: https://fcc.report/IBFS/SAT-MOD-20200417-00037 (accessed on 25 May 2022).
9. OneWeb. Available online: https://oneweb.net/ (accessed on 11 April 2022).
10. Radtke, J.; Kebschull, C.; Stoll, E. Interactions of the space debris environment with mega constellations—Using the example of the OneWeb constellation. *Acta Astronaut.* **2017**, *131*, 55–68. [CrossRef]
11. Reiland, N.; Rosengren, A.J.; Malhotra, R.; Bombardelli, C. Assessing and minimizing collisions in satellite mega-constellations. *Adv. Space Res.* **2021**, *67*, 3755–3774. [CrossRef]
12. Anselmo, L.; Cordelli, A.; Pardini, C.; Rossi, A. Space Debris Mitigation Extension of the SDM Tool. *ISA Tech. Rep. Space Debris* **2000**, *63*. [CrossRef]
13. Virgili, B.B.; Dolado, J.; Lewis, H.; Radtke, J.; Krag, H.; Revelin, B.; Cazaux, C.; Colombo, C.; Crowther, R.; Metz, M. Risk to space sustainability from large constellations of satellites. *Acta Astronaut.* **2016**, *126*, 154–162. [CrossRef]
14. CelesTrak. Available online: https://celestrak.com/ (accessed on 14 December 2021).
15. Stoll, E.; Merz, K.; Krag, H. Ollision Probability Assessment for the Rapideye Satellite Constellation. In Proceedings of the European Conference on Space Debris, Darmstadt, Germany, 22–25 April 2013; p. 9.
16. Tao, H.; Che, X.; Zhu, Q.; Li, X. Satellite In-Orbit Secondary Collision Risk Assessment. *Int. J. Aerosp. Eng.* **2022**, *2022*, 6358188. [CrossRef]
17. Oltrogge, D.L.; Alfano, S. The technical challenges of better Space Situational Awareness and Space Traffic Management. *J. Space Saf. Eng.* **2019**, *6*, 72–79. [CrossRef]
18. Muelhaupt, T.J.; Sorge, M.E.; Morin, J.; Wilson, R.S. Space traffic management in the new space era. *J. Space Saf. Eng.* **2019**, *6*, 80–87. [CrossRef]
19. Lewis, H.G.; Radtke, J.; Rossi, A.; Beck, J.; Oswald, M.; Anderson, P.; Virgili, B.B.; Krag, H. Sensitivity of the space debris environment to large constellations and small satellites. *J. Br. Interplanet. Soc.* **2017**, *70*, 105–117.
20. Kawamoto, S.; Hirai, T.; Kitajima, S.; Abe, S.; Hanada, T. Evaluation of Space Debris Mitigation Measures Using a Debris Evolutionary Model. *Trans. Jpn. Soc. Aeronaut. Space Sci. Aerosp. Technol. Jpn.* **2018**, *16*, 599–603. [CrossRef]
21. Anselmo, L.; Pardini, C. Dimensional and scale analysis applied to the preliminary assessment of the environment criticality of large constellations in LEO. *Acta Astronaut.* **2019**, *158*, 121–128. [CrossRef]
22. Olivieri, L.; Francesconi, A. Large constellations assessment and optimization in LEO space debris environment. *Adv. Space Res.* **2020**, *65*, 351–363. [CrossRef]
23. Union of Concerned Scientists Satellite Database | Union of Concerned Scientists. Available online: https://www.ucsusa.org/resources/satellite-database#.XCcxUVAzbDd (accessed on 1 April 2022).
24. Foust, J. ESA Spacecraft Dodges Potential Collision with Starlink Satellite. Available online: https://spacenews.com/esa-spacecraft-dodges-potential-collision-with-starlink-satellite/ (accessed on 25 November 2021).
25. Aroged Chinese Space Station Nearly Collided with Starlink Satellites Twice-Chinese Unleashed Their Wrath on Musk. Available online: https://www.aroged.com/2021/12/27/chinese-space-station-nearly-collided-with-starlink-satellites-twice-chinese-unleashed-their-wrath-on-musk/ (accessed on 28 December 2021).
26. Braun, V.; Funke, Q.; Lemmens, S.; Sanvido, S. DRAMA 3.0—Upgrade of ESA's debris risk assessment and mitigation analysis tool suite. *J. Space Saf. Eng.* **2020**, *7*, 206–212. [CrossRef]

27. Klinkrad, H. *Space Debris: Models and Risk Analysis*; Springer−Praxis Books in Astronautical Engineering; Springer: Berlin/Heidelberg, Germany; Praxis Pub: Berlin, Germany; New York, NY, USA; Chichester, UK, 2006; ISBN 978-3-540-25448-5.
28. Frey, S.; Colombo, C. Transformation of Satellite Breakup Distribution for Probabilistic Orbital Collision Hazard Analysis. *J. Guid. Control. Dyn.* **2021**, *44*, 88–105. [CrossRef]
29. SDS Space-Track. Available online: https://www.space-track.org (accessed on 11 April 2022).
30. Blandino, J.J.; Martinez, N.; Demetriou, M.; Gatsonis, N.A.; Paschalidis, N. Feasibility for Orbital Life Extension of a CubeSat Flying in the Lower Thermosphere. In Proceedings of the 54th AIAA Aerospace Sciences Meeting, San Diego, CA, USA, 4–8 January 2016. [CrossRef]
31. Bitetti, L.; Ratti, B.B.; Destefanis, R.; Sanchez, A.H. Reliability Model Supporting Satellite Life Extension and Safe Disposal. In Proceedings of the 2018 Annual Reliability and Maintainability Symposium (RAMS), Reno, NV, USA, 22–25 January 2018.